Registry-Induced Electronic Superstructure in Double-Walled Carbon Nanotubes, Associated with the Interaction between Two Graphene-Like Monolayers

Yann Tison,[†] Cristina E. Giusca, Jeremy Sloan,[‡] and S. Ravi P. Silva*

Nano-Electronics Centre, Advanced Technology Institute, University of Surrey, Guildford, Surrey, GU2 7XH, United Kingdom. [†]Present address: Department of Physics, Technical University of Denmark, DK-2800 Kgs. Lyngby, Denmark. [‡]Present address: Department of Physics, University of Warwick, Coventry CV4 7AL, United Kingdom.

ABSTRACT Prior to the implementation of multi-walled carbon nanotubes in microelectronic devices, investigating their electronic structure down to the nanometer scale is necessary. In that prospect, we used scanning tunneling microscopy (STM) to study the detailed atomic scale structure of double-walled carbon nanotubes, each comprising two rolled monolayers of graphene. Atomically resolved STM images usually displayed a motif and periodicity similar to that found in graphite but, on selected regions, atomically resolved motifs with a clearly defined superstructure were observed. This phenomenon has been reported previously but without a suitable explanation. We discuss the origin of this behavior in terms of modified stacking sequences due to the mismatch in registry between the chiral angles of the inner and the outer shells, associated with the interaction between the two carbon monolayers. These phenomena must be taken into account for the realization of lateral interference devices based on carbon nanotubes or graphene layers.

KEYWORDS: double-walled carbon nanotubes · scanning tunneling microscopy · electronic superstructure · interwall interaction · registry mismatch

Research in nanoelectronics has recently been invigorated after the characterization of atomically smooth carbon materials, such as carbon nanotubes[1] or mono- and multilayers of graphene.[2] For instance, several studies demonstrate the possibility of designing field-effect or even single-electron transistors for graphene[3] and single-walled carbon nanotubes (SWNTs).[4,5] Another potential application of these materials is to replace metal stripes as interconnects in the microelectronic industry, especially in the case of multi-walled carbon nanotubes (MWNTs), which have recently been shown to operate at speeds comparable to that of commercial systems.[6] Consequently, many studies, experimental[7−9] as well as theoretical,[10,11] have been undertaken to investigate the detailed relationship between their geometry, their electronic structure, and their transport properties. Double-walled carbon nanotubes (DWNTs) appear to be the perfect model system for this type of investigation, as their two-shell structure gives them the overall properties of larger multi-walled carbon nanotubes and also because their electronic structure is comparatively simpler to analyze than that of multiwall nanotubes consisting of more than two shells. It is now possible to routinely synthesize DWNTs by means of growth methods such as arc-discharge[12] or chemical vapor deposition (CVD)[13] and also by more unique routes which consist of the high-temperature conversion of C_{60}-filled single-walled carbon nanotubes (peapod structures) into double-walled carbon nanotubes.[14] From a structural point of view, high-resolution transmission electron microscopy (HRTEM) studies have demonstrated that the intershell spacing varies between 0.30 and 0.54 nm with a mean value of 0.35 nm.[9,15−17] HRTEM, combined with nanoarea electron diffraction (NAED), also allowed for the determination of the chiral indices for both shells of many DWNTs.[18,19] Recently, the correlation between the structure and the electronic properties in double-walled carbon nanotubes has been investigated using experimental techniques such as *I*(*V*) measurements combined with HRTEM,[9] Raman spectroscopy,[20] nuclear magnetic resonance (NMR),[21] and scanning tunneling microscopy (STM) combined with scanning tunneling spectroscopy (STS).[22,23] These studies highlight the influence of

*Address correspondence to s.silva@surrey.ac.uk.

Received for review July 31, 2008 and accepted September 26, 2008.

Published online October 9, 2008.
10.1021/nn800483k CCC: $40.75

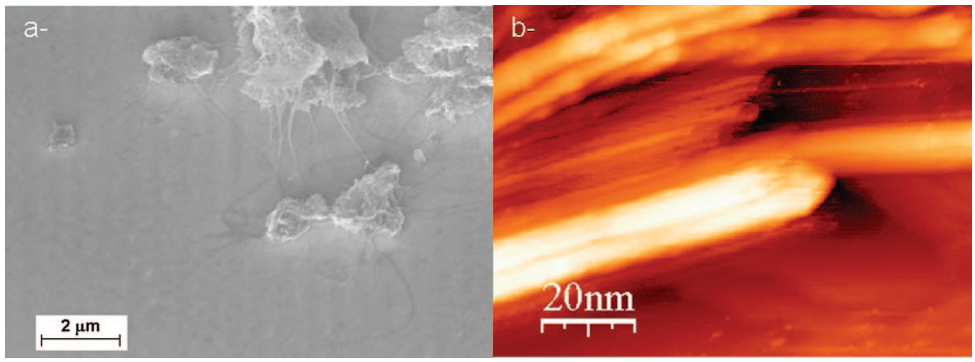

Figure 1. (a) SEM image of aggregates of double-walled carbon nanotubes. Several small bundles can be seen protruding from the aggregate edges. (b) STM image of a bundle of double-walled carbon nanotubes recorded at a sample bias of −165 mV and a tunneling current of 0.100 nA; the *Z*-scale corresponds to 2.9 nm.

both shells on the electronic structure and the transport properties of double-walled carbon nanotubes and, in particular, the presence of an intershell interaction, observations which are also supported by theoretical studies.[24,25] One important aspect for the understanding of this interaction is the lattice registry between the carbon atoms in the inner and the outer shells. Two recent theoretical studies have indicated that, for an inner nanotube with a given conformation, there is an energetically favored outer shell conformation giving rise to an energetically favored inner−outer DWNT pair.[26,27]

In order to help clarifying the structural properties of DWNTs and their consequences on their electronic structure, we present here atomically resolved STM images which show modifications of the periodicity along the tube axis and which bring new insights with regard to the elucidation of the lattice registry effect in DWNTs, in particular, and MWNTs in general.

RESULTS

Double-walled carbon nanotubes were deposited onto a gold substrate, and aggregates and small bundles of tubes could be observed using both scanning electron microscopy (SEM) and scanning tunneling microscopy, as illustrated in Figure 1. On some occasions, isolated DWNTs could also be observed during STM imaging. The DWNTs presented in this report were all tubules located on the periphery of small bundles.

An atomically resolved STM image typical of most of the results we obtained for double-walled carbon nanotubes is shown in Figure 2. The quality of this image is sufficient to allow us to determine the diameter and the chiral angle of its outer shell.

In the case of carbon nanotubes, the accurate determination of these geometrical parameters by STM has been the subject of many discussions in the past decade[28−31] since phenomena such as tip convolution can dramatically affect the measurement. Different models have been developed, based either on the STM tip geometry[28] or the variation of tunneling distance, depending on whether the tip is scanning the nanotube or the substrate.[30] For all the atomically resolved images presented here, we used the method described by Odom *et al.*[31] to determine the chiral angles, and the diameters were calculated by averaging the values extracted from 10 height profiles perpendicular to the tube's axis, as described in a previous report.[22] For the outer shell of the tube presented in Figure 2a, this analysis resulted in values of 21 ± 1° for the chiral angle and 2.06 ± 0.05 nm for the diameter, which corresponds to the chiral indices (19,11).[23] Interestingly, the majority of the STM images we obtained for DWNTs exhibit a 0.25 nm triangular pattern, similar to that of highly oriented pyrolytic graphite (HOPG), as it is highlighted by the height profile and the fast Fourier transform analysis presented in panels b and c of Figure 2, respectively. This pattern

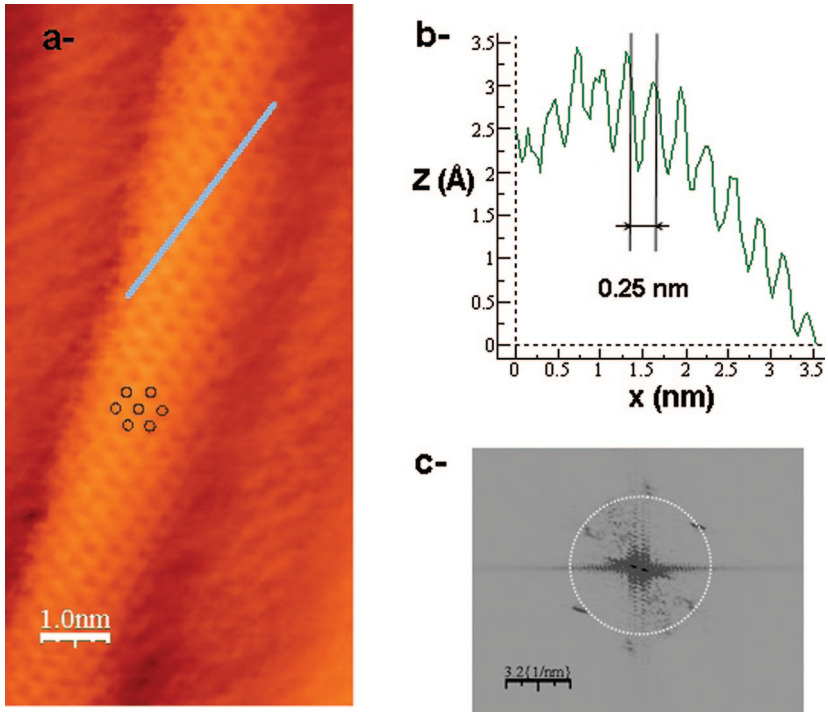

Figure 2. (a) Typical atomically resolved STM image of a double-walled carbon nanotube (sample bias = 230 mV, tunneling current = 0.270 nA, *Z*-scale = 0.6 nm) as presented in ref 23. (b) Height profile recorded along the blue line on the image, highlighting the 0.25 nm triangular lattice. (c) Fast Fourier transform analysis of the image also indicating the presence of a 0.25 nm lattice (the dashed circle corresponds to $k = 4\ \mathrm{nm}^{-1}$ (1/0.25)).

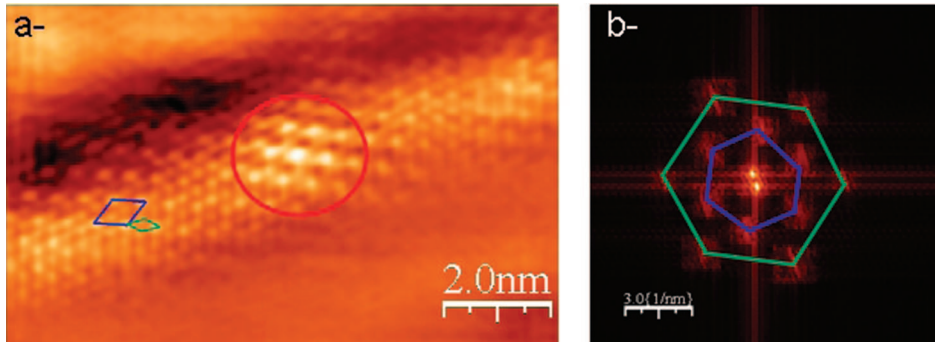

Figure 3. (a) Atomically resolved STM image of a DWNT recorded at a sample bias of −165 mV and a tunneling current of 0.105 nA; the *Z*-scale corresponds to 0.4 nm. This image displays a 0.25 nm triangular lattice highlighted by the green diamond, and the presence of a 0.50 nm lattice rotated by 30° with respect to the latter is highlighted by the blue diamond. A region of higher density of states is also observed in the middle of the image (indicated by the red circle). (b) Two-dimensional fast Fourier transform analysis of the image, where the observation of two hexagons confirms the presence of the 0.25 nm lattice (green) and the 0.50 nm superstructure (blue).

is obtained rather than the 0.14 nm honeycomb lattice usually reported for single-walled carbon nanotubes.[32,33] This unusual imaging behavior has previously been reported for larger multi-walled carbon nanotubes[34] and has been attributed to the predominance of an AB-stacking induced by the presence of an interwall interaction.

Although most of the atomically resolved STM images we obtained for DWNTs are similar to the one presented in Figure 2a and exhibit a regular 0.25 nm triangular lattice, we observed the presence of a superperiodic pattern on several instances. The first example is shown on Figure 3a. Again, we were able to estimate the chiral angle at 5 ± 1° and the diameter at 2.40 ± 0.05 nm, which are associated with the chiral indices (29,3) for the outer shell. In addition to the usual 0.25 nm triangular lattice (indicated by a green diamond in Figure 3a), the image displays an array of brighter spots (highlighted by the blue diamond in Figure 3a). These bright dots form a 0.50 nm superstructure rotated by 30° with respect to the main 0.25 nm lattice ($2 \times 2R30°$). The presence of a superstructure is also clearly indicated by the corresponding fast Fourier transform of the real space image, which displays two hexagons (Figure 3b). The outer hexagon (highlighted in green) is observed at $k = 4$ nm^{-1} in reciprocal space and is associated with the 0.25 nm lattice typical for SWNTs. The inner hexagon (highlighted in blue) corresponds to the 0.50 nm superperiodicity observed for the imaged DWNT. The superstructure is rotated by 30° with respect to the 0.25 nm lattice and appears at $k =$ 2 nm^{-1}. Furthermore, one can distinguish a 2 nm wide area which is characterized by a higher density of states exhibiting the same periodicity as the rest of the image. This region is highlighted by the red circle in Figure 3a.

Another example of a STM image showing a pattern significantly different from the undisturbed 0.25 nm triangular lattice is presented in Figure 4a. In this case, the chiral angle and the diameter of the outer shell have been estimated at 4 ± 1° and 2.70 ± 0.1 nm, respectively. These geometrical parameters are associated with the chiral indices (33,3) or (34,2). A careful inspection of the STM image leads us to divide the area

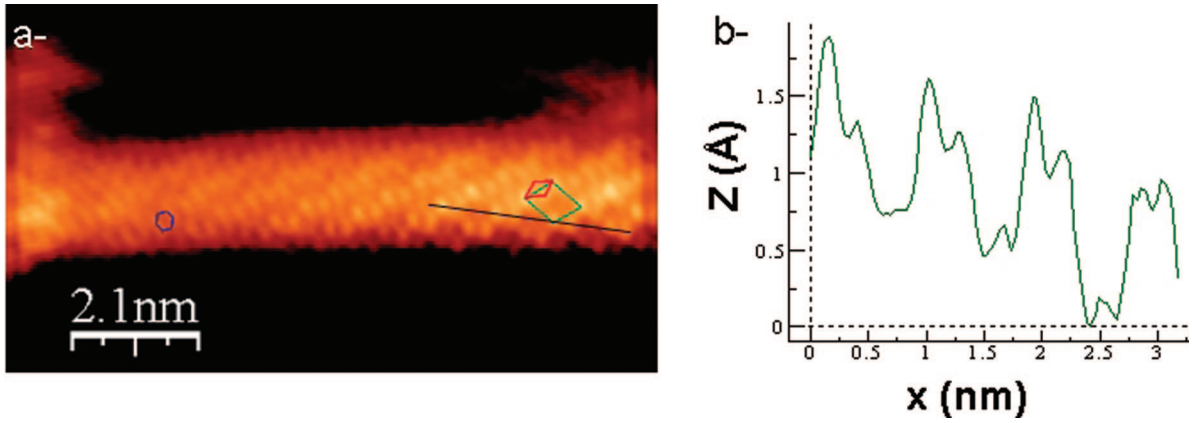

Figure 4. (a) Atomically resolved STM image of a double-walled carbon nanotube (sample bias = +165 mV, tunneling current = 0.103 nA, *Z*-scale = 0.4 nm). The left-hand side of the image displays a 0.14 nm hexagonal array as indicated by the blue hexagon, whereas the right-hand side exhibits a 0.25 triangular lattice (red diamond) superimposed with a 0.50 superstructure (green diamond). (b) Height profile traced along the black line in panel 4a showing that the superstructure pattern is characterized by a succession of bright and dark spots.

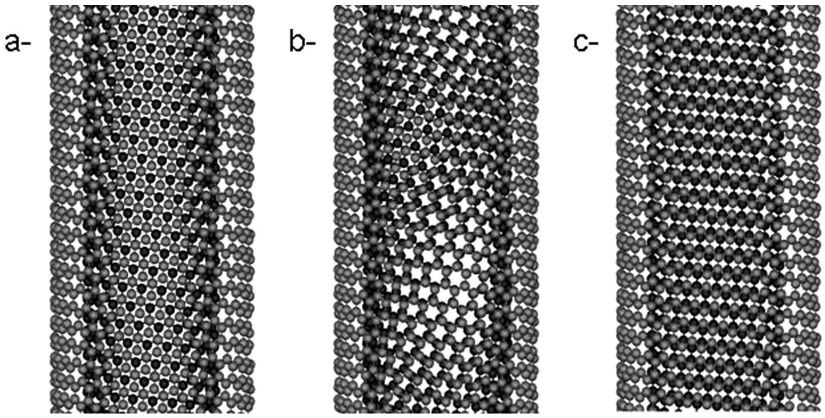

Figure 5. Ball and stick models of (a) a hypothetical double-walled carbon nanotube (19,2@29,3) corresponding to a perfect AB-stacking (for this model structure, the diameter of the inner shell is 1.57 nm and that of the outer shell is 2.40 nm), (b) a hypothetical (20,4@29,3) double-walled carbon nanotube illustrating the case of a mismatch between the chiral angles which induces changes in the local stacking and formation of electronic superstructures (inner tube's diameter = 1.74 nm, outer tube's diameter = 2.40 nm), (c) a (19,2@29,3) DWNT displaying a stacking similar to the one described by Wang *et al.*,[30] which could be associated with areas presenting a 0.14 nm honeycomb lattice. For the three models, the gray balls correspond to carbon atoms belonging to the outer shell, and the black balls to C atoms located in the inner wall (outer tube's diameter = 1.57 nm, inner tube's diameter = 2.40 nm).

under investigation into two regions: (i) on the left-hand side, one can distinguish a 0.14 nm hexagonal pattern similar to that observed in the case of SWNTs; (ii) on the right-hand side of the image and like the image displayed in Figure 3a, this image exhibits a 0.50 nm superstructure superimposed on the 0.25 nm triangular array commonly observed in the case of SWNTs. Again, one observes a rotation of 30° with respect to the 0.25 nm lattice for the superperiodic structure. Figure 4b presents a height profile traced along the indicating black line in Figure 4a and highlights the evolution of the density of states within the superperiodic pattern. This pattern corresponds to a repeating 1D motif consisting of a pair of bright spots, corresponding to a high density of states, followed by a dark area associated with a lower density of states. It is also important to note that the particular tube presented in Figure 4 displays different types of deformations (twist, collapse) which are the subject of another report.[35]

DISCUSSION

STM experiments have been performed on DWNTs, and several results show data that are unexpected and not usually observed for either hexagonal graphene-like layers of carbon or for SWNTs. First, most of the STM images of DWNTs display a triangular array with a lattice parameter of 0.25 nm. This periodicity is different from the honeycomb lattice with an interatomic distance of 0.14 nm obtained in the case of SWNTs,[32,33] although this has also been reported for larger MWNTs.[34] The presence of a 0.25 nm triangular lattice probably indicates a behavior similar to that observed in the case of HOPG, for which the 0.25 nm triangular lattice of the STM image arises from both its geometrical and electronic structures.[36] At the surface of AB-stacked HOPG, 50% of the surface carbon atoms are located above a carbon atom belonging to the underlying layer (site A), whereas the other carbon atoms are situated on top of a vacancy (site B). Due to a $\pi-\pi$ interaction, a gap opens between the π and π^* electronic states for the carbon atoms located in sites A. Therefore, the density of states at the Fermi edge corresponding to the carbon atoms in sites A is negligible compared to that of the carbon atoms in sites B, and only B-type carbon atoms are observed in the STM image. Hence, one can reasonably conclude that the similarity between the periodicity generally observed on the STM images of DWNTs and that reported in the case of HOPG suggests that carbon atoms in DWNTs would be arranged in a similar fashion to the AB-stacking of HOPG, with slight modifications due to the nanotube curvature, as displayed in Figure 5a. This observation is also consistent with recent STM images of double layers of graphene which show a similar triangular pattern with a 0.25 nm lattice parameter, whereas the images obtained for single layers display a honeycomb motif with an interatomic distance of 0.14 nm,[37,38] as it is the case for single-walled carbon nanotubes.[32,33]

However, the superstructures observed in the STM image in Figures 3a and in the right-hand side of Figure 4a demonstrate that the AB-stacking is not perfect. To explain this behavior, one should be reminded that HRTEM combined with NAED experiments recently demonstrated that the chiral angles of the inner and the outer shells are not directly correlated and can be effectively incommensurate.[18,19] Such a mismatch can induce the formation of an electronic superstructure associated with an AB-stacking close to registry, similar to that of a moiré pattern in the case of graphite.[39] Many hypotheses have been formulated to explain the presence of moiré patterns on the STM images of graphite. It is currently accepted that the superlattice corresponding to this effect arises from a rotation of the topmost graphene sheet with regard to the underlying layers.[39] This conformation induces periodical variations of the density of states in the vicinity of the Fermi edge which can be detected using STM. However, as highlighted by Ge and Sattler[40] in an early STM study of multi-walled carbon nanotubes, the moiré pattern observed in graphite is extended throughout the whole surface of the topmost layer, whereas the geometry of the DWNTs imaged in the present study confines the formation of a superlattice to localized areas on the surface of the nanotube due to the shell curvature. This is a significant result, as it confirms the models suggesting that just two layers of graphene can give rise to ex-

tended periodical structures as sound in 3D crystals due to the highly coupled nature of the electronic wave function between the layers.[41] The results further highlight the potential of carbon systems, such as double-layered graphene, to be able to produce interesting interference phenomena, despite having only two layers of atomically thin material interacting with each other.

Another point of interest is the change of periodicity observed along the DWNT presented on Figure 4. The right-hand side exhibits a structure induced electronic superlattice similar to that shown on Figure 3, associated with an imperfect AB-stacking. The left-hand side of the image, however, displays a honeycomb lattice with a 0.14 nm interatomic distance. Such a pattern is regularly observed in the case of single-walled carbon nanotubes, and one could conclude that the inner shell does not extend to this part of the DWNT. However, STM images recorded further to the left for the same tube[35] show a 0.25 nm periodicity, indicating the presence of two shells. Therefore, we believe that this nanotube is indeed constituted of two shells over its entire length, and the 0.14 nm honeycomb lattice can be attributed to a particular arrangement of the concentric shells. Recently, a similar pattern has been reported for graphite, and it has been associated with a particular type of stacking which corresponds to a sliding of the topmost graphene sheet by 0.071 nm along the *a* axis of the hexagonal cell,[41] as shown on Figure 5c. Furthermore, AA-type stacking could also be responsible for such a periodicity, as all the surface carbon atoms would be crystallographically equivalent. Considering the mismatch between the chiral angles of the two shells, one can imagine a transition between an imperfect AB-stacking sequence, responsible for the 0.25 nm triangular lattice with a superstructure, and a conformation similar to that of Figure 5c, which would lead to the observation of a honeycomb lattice on the STM image. Another point to mention here is the presence of deformations such as twist and collapse[35] in other areas of this tube, which could also be one of the parameters involved in the change of periodicity observed on Figure 4a.

The above considerations, if they correctly describe the formation of the images presented in Figures 3 and 4, do not account for the observation of an undisturbed 0.25 nm triangular lattice on the majority of the images we have obtained for DWNTs (Figure 2). As the energy barrier for the rotation of one tube relative to the other is extremely small[42,43] and the AB-stacked graphite is the most stable form of graphite,[44] the two shells can rotate in order to minimize the double-walled carbon nanotube total energy or, in other words, to maximize the total area exhibiting AB-stacking. Hence, from a statistical point of view, most of the STM images obtained for DWNTs correspond to an AB-stacked region and display a 0.25 nm triangular lattice. This argument is also supported by the variation of interwall distance in a DWNT,[9,15−17] which could correspond to the distortion of one of the constituent tubes in order to maximize the area associated with an AB-stacking sequence.

Recently, lattice registry-dependent potentials have been developed in an attempt to describe the interaction between the shells of multi-walled carbon nanotubes more accurately.[26,45] When applied to double-walled carbon nanotubes, this approach helped demonstrate that some couples of chiral indices are energetically favored with regard to the other possible combinations.[26,27] In the case of DWNTs with large diameters, it was reported that the chiral angles of the outer and the inner shells are very similar, which is in agreement with the observation of monochiral MWNTs grown at low temperatures.[46] For smaller DWNTs, there is a significant mismatch between the chiral angles corresponding to the walls of the most energetically favored chiral combination.[27] Therefore, the presence of regions exhibiting different types of stacking is likely to be observed. In our opinion, these optimum chiral combinations correspond to cases for which the surface of the AB-stacked areas can be maximized. However, this hypothesis is limited by two observations. First, one should remember that the dominance of the energetically favored DWNTs must be understood in terms of probability and that all the other possible cases can be observed, as the energy difference between the most stable chiral combination and all the other possibilities is smaller than 5 meV/atom.[27] Second, HRTEM results show that there is no systematic correlation between the chiral angles of the two shells in a DWNT.[18,19]

The presence of a region of higher density of states on the STM image presented on Figure 3a is also of interest. It seems that this feature does not arise from a defect belonging to the top-side of the outer shell of the double-walled carbon nanotube as its pattern and periodicity are not different from those of the whole image. Indeed, topological defects such as pentagon−heptagon pairs would lead to a change of chirality along the tube,[47] which is not observed in this particular case. Defects generated by Ar^+ irradiation could locally lead to the formation of a superlattice in the case of large MWNTs,[48] but they usually appear as hillocks on the nanotube surface, structures which were not observed in the case of the DWNTs decribed in this study. This higher density of states could also be a consequence of either the mismatch between the chiral angles as discussed earlier by Ge and Sattler[40] or the presence of a localized defect in the inner shell. The influence of a feature belonging to the gold substrate, such as a monatomic step, should not be neglected, as it could affect the local density of states of the DWNTs.

The presence of electronic superstructure on the STM images of DWNTs shows that the surface density of states in the vicinity of the Fermi edge can be affected by the presence of the underlying shell. The

theoretical study of a STM image of graphite which exhibits a moiré pattern demonstrated that small changes in the local stacking sequence could lead to important variations of density of states at the Fermi level and to the contrast fluctuations observed on the STM image.[49] Although further theoretical modeling is needed to fully understand the formation of moiré patterns in STM, it seems that this effect is related to the interlayer interaction in graphite.[39] Therefore, the observation of superperiodical patterns on the STM image of DWNTs gives evidence of the presence of an intershell interaction in DWNTs. The consequences of the interwall interaction on the transport properties of multi-walled carbon nanotubes have been widely investigated in the past decade. From a theoretical point of view, tight-binding models predict that the electronic intertube transfer induced by this interaction can be neglected while describing the transport properties of DWNTs, and MWNTs by extension,[10] whereas DFT calculations evidence significant charge transfers and intershell conductance.[11,24] Experimentally, early studies suggested that the current flows only through the outermost layer of MWNTs.[7] However, more recent work, based on the removal of the outermost layer, demonstrated that many layers are involved in the electron transport,[8] due to the presence of an interwall interaction. Coming back to double-walled carbon nanotubes, the registry-induced electronic superstructure presented here, and STS results which suggest that double-walled carbon nanotubes with a semiconducting outer shell can display a metallic behavior,[22,23] clearly demonstrate that the inner shell has to be taken into account in order to describe the surface electronic structure of a DWNT and that the intershell coupling cannot be neglected. Consequently, one has to consider the electronic structure of a multi-walled carbon nanotube as a whole complex structure and not as the sum of the electronic structure of noninteracting concentric single-walled carbon nanotubes. The results we recently obtained for double-walled carbon nanotubes may imply that these structures present a metallic behavior by nature because of the intershell interaction. As a consequence, they would be a better choice than single-walled carbon nanotubes for a use as interconnects in micro- or nanoelectronics, as two-thirds of the SWNTs are semiconducting from a statistical point of view and, therefore, not suitable for this type of application. Furthermore, our observations could help refine the theoretical models which lead to contradictory results, depending on the formalism. For instance, a tight-binding approach suggests that a combination of two concentric semiconducting SWNTs cannot lead to a metallic DWNT,[50] whereas an opposite behavior is observed after a recent DFT calculation.[25]

To conclude, different types of patterns and periodicities observed in STM images obtained from DWNTs are described in this paper. The images usually display a triangular array with a lattice parameter of 0.25 nm, but a honeycomb lattice with a 0.14 nm interatomic distance can also be observed. Furthermore, we observed the presence of registry-induced superstructures based on the 0.25 nm triangular lattice on several occurences. This behavior shows that the shells of a double-walled carbon nanotube can be stacked in different ways such as AB, AA, or more complicated configurations. A model is proposed to rationalize these observations in terms of the difference of chiral angles between the shells, of the free rotation of a shell relative to the other, and of the relative stabilities of the different stacking sequences of graphite. In our opinion, only the combination of HRTEM and atomically resolved STM imaging would give access to both the atomic positions in the different shells and to the surface density of states with subnanometer resolution and thus highlight the relationship between the stacking sequence and the formation of superstructures. Furthermore, electronic structure theoretical calculations, combined with a modeling of the STM image, will be necessary in order to fully describe the formation of the electronic superstructures observed on the STM images of DWNTs. Finally, the data further confirm that the coupling between the shells of carbon nanotubes is stronger than previously considered. Our observations also have significant impact on the theoretical and experimental fabrication of new types of devices, based on interacting graphene layers, which could utilize the electronic superstructures.

METHODS

The double-walled carbon nanotubes used in this work have been purchased from Carbon Nanotechnologies Incorporated. Prior to the experiment, the nanotubes have been acid treated (reflux in HNO_3, 2 mol · L^{-1}, 150 °C for 24 h followed by a reflux in HCl, 2 mol · L^{-1}, 150 °C for 45 min) and oxidized in air (300 °C, 1 h) in order to remove most of the catalyst and amorphous carbon impurities. The purified DWNTs were then dispersed in 1,2-dichloroethane (1 mg · mL^{-1}) and sonicated for 2 h prior STM experiments being performed. TEM experiments were also realized in order to check the quality of the sample (number of walls, absence of amorphous carbon), and the results have been reported elsewhere.[22] To prepare the STM sample, a few drops of the sonicated dispersion were deposited on a gold(111) surface. The sample was then mounted on a sample plate and introduced into the ultrahigh vacuum scanning tunneling microscope (UHV-STM).

STM and STS experiments were performed at room temperature in a commercial UHV-STM (Omicron VT Multiscan STM) equipped with a SEM column. The calibration of the STM was regularly tested against HOPG, and STM images showed the correct periodicity and lattice parameters. The experimental error is estimated at ±0.01 nm from these measurements. Electrochemically etched tungsten tips have been used for this study. During the experiments, the base pressure in the UHV chamber was better than 3×10^{-11} mbar. STM images were recorded in

constant current mode with the sample biased in the range of −0.3 to 0.3 V and the tunneling current maintained at approximately 100 pA. The STM images were processed and analyzed using the WSxM package.[51]

Acknowledgment. We thank Y. Hayashi, Nagoya Institute of Technology, Japan, for providing the double-walled carbon nanotubes, and E. Borowiak-Palen, Szczecin University of Technology, Poland, for her help in the purification of nanotubes. This work was funded by EPSRC in the form of a Portfolio Partnership award.

REFERENCES AND NOTES

1. Iijima, S. Helical Microtubules of Graphitic Carbon. *Nature* **1991**, *354*, 56–58.
2. Novoselov, K. S.; Geim, A. K.; Morozov, S. V.; Jiang, D.; Zhang, Y.; Dubonos, S. V.; Grigorieva, I. V.; Firsov, A. A. Electric Field in Atomically Thin Carbon Films. *Science* **2004**, *306*, 666–669.
3. Lemme, M. C.; Echtemeyer, T. J.; Baus, M.; Kurz, H. A Graphene Field Effect Device. *IEEE Electron Device Lett.* **2007**, *28*, 282–284.
4. Postma, H. W. Ch.; Teepen, T.; Yao, Z.; Grifoni, M.; Dekker, C. Carbon Nanotube Single Electron Transistors at Room Temperature. *Science* **2001**, *293*, 76–79.
5. Chen, Z.; Appenzeller, J.; Lin, Y.-M.; Sippel-Oakley, J.; Rinzler, A. G.; Tang, J.; Wind, S. J.; Solomon, P. M.; Avouris, P. An Integrated Logic Circuit Assembled on a Single Carbon Nanotube. *Science* **2006**, *311*, 1735.
6. Close, G. F.; Yasuda, S.; Paul, B.; Fujita, S.; Wong, H.-S. P. 1 GHz Integrated Circuit with Carbon Nanotube Interconnects and Silicon Transistor. *Nano Lett.* **2008**, *8*, 706–709.
7. Frank, S.; Poncharal, P.; Wang, Z. L.; de Heer, W. A. Carbon Nanotube Quantum Resistors. *Science* **1998**, *280*, 1744–1746.
8. Collins, P. G.; Avouris, P. Multishell Conduction in Multiwalled Carbon Nanotubes. *Appl. Phys. A* **2002**, *74*, 329–332.
9. Kociak, M.; Suenaga, K.; Hirahara, K.; Saito, Y.; Nakahira, T.; Iijima, S. Linking Chiral Indices and Transport Properties of Double-Walled Carbon Nanotubes. *Phys. Rev. Lett.* **2002**, *89*, 155501-1–155501-4.
10. Uryu, S.; Ando, T. Electronic Intertube Transfer in Double-Wall Carbon Nanotubes. *Phys. Rev. B* **2005**, *72*, 245403-1–245403-10.
11. Hansson, A.; Stafström, S. Intershell Conductance in Multiwall Carbon Nanotubes. *Phys. Rev. B* **2003**, *67*, 075406-1–075406-6.
12. Hutchison, J. L.; Kiselev, N. A.; Krinichnaya, E. P.; Krestinin, A. V.; Loufty, R. O.; Morawski, A. P.; Muradyan, V. E.; Obratzova, E. D.; Sloan, J.; Terekhov, S. V.; et al. Double-Walled Carbon Nanotubes Fabricated by a Hydrogen Arc Discharge Method. *Carbon* **2001**, *39*, 761–770.
13. Ren, W.; Li, F.; Chen, J.; Bai, S.; Cheung, H. M. Morphology, Diameter Distribution and Raman Scattering Measurements of Double-Walled Carbon Nanotubes Synthesized by Catalytic Decomposition of Methane. *Chem. Phys. Lett.* **2002**, *359*, 196–202.
14. Bandow, S.; Takizawa, M.; Hirahara, K.; Yudasaka, M.; Iijima, S. Raman Scattering Study of Double-Wall Carbon Nanotubes Derived from the Chains of Fullerenes in Single-Wall Carbon Nanotubes. *Chem. Phys. Lett.* **2001**, *337*, 48–54.
15. Kociak, M.; Hirahara, K.; Suenaga, K.; Iijima, S. How Accurate Can the Determination of Chiral Indices of Carbon Nanotubes Be? An Experimental Investigation of Chiral Indices Determination on DWNT by Electron Diffraction. *Eur. Phys. J. B* **2003**, *32*, 457–469.
16. Zhu, H.; Suenaga, K.; Hashimoto, A.; Urita, K.; Iijima, S. Structural Identification of Single and Double-Walled Carbon Nanotubes by High-Resolution Transmission Electron Microscopy. *Chem. Phys. Lett.* **2005**, *412*, 116–120.
17. Costa, P. M. F. G.; Friedrichs, S.; Sloan, J.; Green, M. L. H. Structural Studies of Purified Double Walled Carbon Nanotubes (DWNTs) Using Phase Restored High-Resolution Imaging. *Carbon* **2004**, *42*, 2527–2533.
18. Zuo, J. M.; Vartanyants, I.; Gao, M.; Zhang, R.; Nagahara, L. A. Atomic Resolution Imaging of a Carbon Nanotube from Diffraction Intensities. *Science* **2003**, *300*, 1419–1421.
19. Hashimoto, A.; Suenaga, K.; Urita, K.; Shimada, T.; Sugai, T.; Bandow, S.; Shinohara, H.; Iijima, S. Atomic Correlation between Adjacent Graphene Layers in Double-Wall Carbon Nanotubes. *Phys. Rev. Lett.* **2005**, *94*, 045504-1–045504-4.
20. Pfeiffer, R.; Simon, F.; Kuzmany, H.; Popov, V. N.; Zólyomi, V.; Kürti, J. Tube−Tube Interaction in Double-Wall Carbon Nanotubes. *Phys. Status Solidi B* **2006**, *243*, 3268–3272.
21. Singer, P. M.; Wzietek, P.; Alloul, H.; Simon, F.; Kuzmany, H. NMR Evidence for Gapped Spin Excitations in Metallic Carbon Nanotubes. *Phys. Rev. Lett.* **2005**, *95*, 236403-1–236403-4.
22. Giusca, C. E.; Tison, Y.; Stolojan, V.; Borowiak-Palen, E.; Silva, S. R. P. Inner-Tube Chirality Determination for Double-Walled Carbon Nanotubes by Scanning Tunneling Microscopy. *Nano Lett.* **2007**, *7*, 1232–1239.
23. Tison, Y.; Giusca, C. E.; Stolojan, V.; Hayashi, Y.; Silva, S. R. P. The Inner Shell Influence on the Electronic Structure of Double-Walled Carbon Nanotubes. *Adv. Mater.* **2008**, *20*, 189–194.
24. Miyamoto, Y.; Saito, S.; Tománek, D. Electronic Interwall Interactions and Charge Redistribution in Multiwall Nanotubes. *Phys. Rev. B* **2002**, *65*, 041402-1–041402-4.
25. Zólyomi, V.; Rusznyák, Á.; Kürti, J.; Gali, Á.; Simon, F.; Kuzmany, H.; Szabados, Á.; Surján, P. R. Semiconductor-to-Metal Transition of Double Walled Carbon Nanotubes Induced by Inter-Shell Interaction. *Phys. Status Solidi B* **2006**, *243*, 3476–3479.
26. Bellarosa, L.; Bakalis, E.; Melle-Franco, M.; Zerbetto, F. Interactions in Concentric Carbon Nanotubes: the Radius *vs* the Chirality Angle Contributions. *Nano Lett.* **2006**, *6*, 1950–1954.
27. Guo, W.; Guo, Y. Energy Optimum Chiralities of Multiwalled Carbon Nanotubes. *J. Am. Chem. Soc.* **2007**, *129*, 2730–2731.
28. Venema, L. C.; Meunier, V.; Lambin, Ph.; Dekker, C. Atomic Structure of Carbon Nanotubes from Scanning Tunneling Microscopy. *Phys. Rev. B* **2000**, *61*, 2991–2996.
29. Meunier, V.; Lambin, Ph. Tight-Binding Computation of the STM Image of Carbon Nanotubes. *Phys. Rev. Lett.* **1998**, *81*, 5588–5591.
30. Kim, P.; Odom, T. W.; Huang, J. L.; Lieber, C. M. STM Study of Single-Walled Carbon Nanotubes. *Carbon* **2000**, *38*, 1741–1744.
31. Odom, T. W.; Huang, J. L.; Kim, P.; Ouyang, M.; Lieber, C. M. Scanning Tunneling Microscopy and Spectroscopy Studies of Single Wall Carbon Nanotubes. *J. Mater. Res.* **1998**, *13*, 2380–2388.
32. Wildöer, J. W. G.; Venema, L. C.; Rinzler, A. G.; Smalley, R. E.; Dekker, C. Electronic Structure of Atomically Resolved Carbon Nanotubes. *Nature* **1998**, *391*, 59–62.
33. Odom, T. W.; Huang, J. L.; Kim, P.; Lieber, C. M. Atomic Structure and Electronic Properties of Single-Walled Carbon Nanotubes. *Nature* **1998**, *391*, 62–64.
34. Hassanien, A.; Mrzel, A.; Tokumoto, M.; Tomànek, D. Imaging the Interlayer Interactions of Multiwall Carbon Nanotubes Using Scanning Tunneling Microscopy and Spectroscopy D. *Appl. Phys. Lett.* **2001**, *79*, 4210–4212.
35. Giusca, C. E., Tison, Y., Silva, S. R. P. Evidence for Metal-Semiconductor Transitions in Twisted and Collapsed Double-Walled Carbon Nanotubes by Scanning Tunnelling Microscopy *Nano Lett.* **2008**, in press.
36. Magonov, S.; Whangbo, M.-H. *Surface Analysis with STM and AFM* VCH: Weinhem, Germany, 1996; pp 77−80.
37. Stolyarova, E.; Rim, K. T.; Ryu, S.; Maultzsch, J.; Kim, P.; Brus, L. E.; Heinz, T. F.; Hybertsen, M. S.; Flynn, G. W. High-Resolution Scanning Tunneling Microscopy Imaging of

Mesoscopic Graphene Sheets on an Insulating Surface. *Proc. Natl. Acad. Sci. U.S.A.* **2007**, *104*, 9209–9212.
38. Brar, V. W.; Zhang, Y.; Yavon, Y.; Ohta, T.; McChesney, J. L.; Bostwick, A.; Rotenberg, E.; Horn, K.; Crommie, M. F. Scanning Tunneling Spectroscopy of Inhomogeneous Electronic Structure in Monolayer and Bilayer Graphene on SiC. *Appl. Phys. Lett.* **2007**, *91*, 122102-1–122102-3.
39. Pong, W.-T.; Bendall, J.; Durkan, C. Observation and Investigation of Graphite Superlattice Boundaries by Scanning Tunneling Microscopy. *Surf. Sci.* **2007**, *601*, 498–509.
40. Ge, M.; Sattler, K. Vapor-Condensation Generation and STM Analysis of Fullerene Tubes. *Science* **1993**, *260*, 515–518.
41. Wang, Y.; Ye, Y.; Wu, K. Simultaneous Observation of the Triangular and Honeycomb Structures on Highly Oriented Pyrolytic Graphite at Room Temperature: An STM Study. *Surf. Sci.* **2006**, *600*, 729–734.
42. Charlier, J.-C.; Michenaud, J.-P. Energetics of Multilayered Carbon Tubules. *Phys. Rev. Lett.* **1993**, *70*, 1858–1861.
43. Bitchouskaya, E.; Heggie, M. H.; Popov, A. M.; Lozovik, Y. E. Interwall Interaction and Elastic Properties of Carbon Nanotubes. *Phys. Rev. B* **2006**, *73*, 045435-1–045435-9.
44. Omata, Y.; Yamagami, Y.; Tadano, K.; Miyake, T.; Saito, S. Nanotube Nanoscience: A Molecular-Dynamics Study. *Physica E* **2005**, *29*, 454–468.
45. Kolmogorov, A. N.; Crespi, V. H. Registry-Dependent Interlayer Potential for Graphitic Systems. *Phys. Rev. B* **2005**, *71*, 235415-1–235415-6.
46. Xu, Z.; Bai, X.; Wang, Z. L.; Wang, E. Multiwall Carbon Nanotubes Made of Monochirality Graphite Shells. *J. Am. Chem. Soc.* **2006**, *128*, 1052–1053.
47. Ouyang, M.; Huang, J.-L.; Cheung, C. L.; Lieber, C. M. Atomically Resolved Single-Walled Carbon Nanotube Intramolecular Junctions. *Science* **2001**, *291*, 97–100.
48. Osváth, Z.; Vértesy, G.; Tapasztó, L.; Wéber, F.; Horváth, Z. E.; Gyulai, J.; Biró, L. P. Atomically Resolved STM Images of Carbon Nanotube Defects Produced by Ar^+ Irradiation. *Phys. Rev. B* **2005**, *72*, 045429-1–045429-6.
49. Rong, Z. Y.; Kuiper, P. Electronic Effects in Scanning Tunneling Microscopy: Moiré Pattern on a Graphite Surface. *Phys. Rev. B* **1993**, *48*, 17427–17431.
50. Saito, R.; Dresselhaus, G.; Dresselhaus, M. S. Electronic Structure of Double-Layer Graphene Tubules. *J. Appl. Phys.* **1993**, *73*, 494–500.
51. Horcas, I.; Fernandez, R.; Gomez-Rodriguez, J. M.; Colchero, J.; Gomez-Herrero, J.; Baro, A. M. WSxM: A Software for Scanning Probe Microscopy and a Tool for Nanotechnology. *Rev. Sci. Instrum.* **2007**, *78*, 013705-1–013705-8.